Z. Phys. C - Particles and Fields 23, 103–109 (1984)

Zeitschrift für Physik C Particles and Fields

New Data on Semihadronic Decays of the τ Lepton

CELLO-Collaboration

H.J. Behrend, H. Fenner, M.-J. Schachter[1], V. Schröder, H. Sindt

Deutsches Elektronen-Synchrotron, DESY, D-2000 Hamburg, Federal Republic of Germany

O. Achterberg, G. D'Agostini, W.-D. Apel, J. Engler, G. Flügge, B. Forstbauer, D.C. Fries, W. Fues, K. Gamerdinger, Th. Henkes, G. Hopp, M. Krüger, H. Küster, H. Müller, H. Randoll[2], G. Schmidt[3], H. Schneider

Kernforschungszentrum Karlsruhe and Universität, D-7500 Karlsruhe, Federal Republic of Germany

W. de Boer, G. Buschhorn, G. Grindhammer, P. Grosse-Wiesmann[4], B. Gunderson, C. Kiesling, R. Kotthaus, U. Kruse[5], H. Lierl[6], D. Lüers, H. Oberlack, P. Schacht, W. Wiedenmann

Max-Planck-Institut für Physik und Astrophysik, D-8000 München, Federal Republic of Germany

G. Bonneaud[7], P. Colas, A. Cordier, M. Davier, D. Fournier, J.F. Grivaz, J. Haissinski, V. Journé, F. Laplanche, F. Le Diberder, U. Mallik[8], E. Ros, J.-J. Veillet

Laboratoire de l'Accélérateur Linéaire, F-91405 Orsay, France

J.H. Field[9], R. George, M. Goldberg, B. Grossetête, O. Hamon, F. Kapusta, F. Kovacs, G. London, R. Pain, L. Poggioli, M. Rivoal

Laboratoire de Physique Nucléaire et Hautes Energies, University, F-75230 Paris, France

R. Aleksan, J. Bouchez, G. Carnesecchi[10], G. Cozzika, Y. Ducros, A. Gaidot, P. Jarry, Y. Lavagne, J. Pamela, J.P. Pansart, F. Pierre

Centre d'Etudes Nucléaires, Saclay, F-91190 Gif-sur-Yvette, France

Received 13 February 1984

Abstract. Branching ratios for the decay $\tau \to \nu + (n$ pions) with $n \geqq 2$ are presented. The new data include all possible charge configurations of the pion system and, in particular, final states containing one or several neutral pions. The data are compared with predictions from CVC (even number of pions in final state) and current algebra (odd number of pions). They strongly support the standard coupling of the τ to the weak charged current.

1 Now at SCS, Hamburg, FRG
2 Now at Blaupunkt, Hildesheim, FRG
3 Now at Siemens, München, FRG
4 Now at Universität Karlsruhe, FRG
5 Now at University of Illinois, Urbana, USA
6 Now at DESY, Hamburg, FRG
7 CRN, Strasbourg, France
8 Now at Purdue University, W. Lafayette, USA
9 On leave of absence from DESY, Hamburg, FRG
10 Now at CRAY Research, Paris, France

Introduction

τ leptons from $e^+ e^-$ annihilations have proven a useful tool for testing various aspects of the Standard Model of electroweak interactions [1] through charge asymmetry [2, 3] and polarization measurements [4]. In all these analyses the τ was assumed to couple to the conventional $V-A$ charged current. Experiments on the τ decay properties carried out so far have supported this idea: The major branching ratios [4, 5], decay lepton spectra [6], and the τ life time [7] are consistent with the standard $V-A$ coupling. Very little [8] or not data exist, however, on a large fraction ($\sim 30\%$) of the τ decay channels, i.e. decays into several pions + neutrino. On the other hand rather firm theoretical predictions exist for the width into an even number of pions from $e^+ e^- \to 2n$ pions using only the CVC hypothesis [9], and, to a lesser extent, on the width into an odd number of

pions using current algebra and PCAC [9, 10]. The main experimental difficulty which may have delayed an earlier mesurement of these channels is connected to the (potential) presence of neutral pions among the final state hadrons. For an even number of pions one always has at least one neutral pion in the final state. Furthermore one has to make sure that a system containing only charged pions is not contaminated by events with undetected π^0's. Thus good neutral detection is mandatory. In this letter we report on measurements of the following decay channels (τ^- is used symbolically for both charge states):

$$\tau^- \to \pi^- \pi^0 \nu \quad (1)$$

$$\tau^- \to \pi^- \pi^0 \pi^0 \nu \quad (2)$$

$$\tau^- \to \pi^- \pi^0 \pi^0 \pi^0 \nu \quad (3)$$

$$\tau^- \to \pi^- \pi^+ \pi^- \nu \quad (4)$$

$$\tau^- \to \pi^- \pi^+ \pi^- \pi^0 \nu \quad (5)$$

$$\tau^- \to \pi^- \pi^+ \pi^+ \pi^- \pi^- \nu \quad (6)$$

The data were recorded by the CELLO detector at PETRA, running at moderate energies (14 and 22 GeV CMS energy). At these energies τ final states containing many pions suffer less from overlap problems (see below) and are thus easier to analyze. We will briefly describe the experiment and then turn to the event selection and the analysis of the multipion final states from the τ decay. The measured branching ratios will be compared to predictions from $e^+e^- \to$ hadrons using CVC, and to predictions from current algebra.

Experiment

The experiment was performed using the CELLO detector at PETRA. We briefly mention the detector components relevant for this analysis, a more detailed description of CELLO can be found elsewhere [11]. The momentum of charged particles is measured in a solenoidal magnetic spectrometer equipped with a superconducting magnet of 1.31 T and 12 layers of cylindrical drift- and proportional chambers. It covers the polar range of $|\cos\theta| < 0.91$. Using the vertex constraint we achieve, for Bhabha events, a momentum resolution of $\Delta p/p = 1.7\% p$ [GeV]. Photons and electrons are identified in a fine grain barrel liquid argon calorimeter which covers $|\cos\theta| < 0.86$, and liquid argon endcaps covering $0.93 < \cos\theta < 0.99$. The energy deposition is sampled in 6 layers up to a maximum depth of 20 radiation lengths (X_0) at 90°. Each layer consists of channels in 3 orientations. We obtain an energy resolution of $\Delta E/E = 13\%/\sqrt{E}$ [GeV] and an angular resolution of 4 mrad. Photons as low as 100 MeV can be measured with an efficiency of $\sim 50\%$.

Muons are detected in planar proportional chambers surrounding the detector behind 5 to 8 absorption lengths of iron. They cover 92% of 4π. Our trigger logic incorporated a two-charged-particle trigger with a momentum cut-off at 250 MeV/c, various calorimetric triggers and combinations of charged and calorimetric triggers. The luminosity was determined with Bhabha events in the barrel and was cross-checked with Bhabha scattering in the end cap region of the detector. Data were taken at $\sqrt{s} = 14$ and 22 GeV with an integrated luminosity of 1.0 and 2.5 pb^{-1}, respectively.

Event Selection

In order to select τ pairs from the events recorded by CELLO, the event topology is defined using the sphericity axis calculated from all observed charged prongs and neutral particles. Events with energy deposition in the endcaps in excess of 3 GeV were rejected. The particles are divided into two jets by the plane perpendicular to the sphericity axis. For each hemisphere the normalized momentum vector sum $\mathbf{n}_i$ of all charged particles, the total charge Q_i and the total invariant mass m_i (including neutrals and assuming pions for the charged particles) is calculated. The true charged multiplicity in each hemisphere is restored by identifying electron-positron pairs from γ conversions in the beampipe or in the chambers. This has been achieved by reconstructing the true conversion point and forming the invariant mass with the re-evaluated kinematical quantities at the conversion point. A mass cut of 80 MeV was employed to define an e^+e^- pair. The pairs thus found were taken out of the charged multiplicity and counted as photons in the subsequent analysis. Events are accepted with a total charged multiplicity < 10 and a minimum energy deposit of 360 MeV in at least one jet. For the 2 prong topology we require the polar angle θ to satisfy $|\cos\theta| < 0.85$ for each of the oppositely charged particles. Electrons were identified via their characteristic shower pattern in the calorimeter ($> 60\%$ of the energy deposited in the first 2 lead layers of the calorimeter, corresponding to an average of $5 X_0$) and by comparing the total energy deposited with the measured particle momentum. The efficiency for identifying electrons is around 80% beyond 2 GeV. 2 prongs with 2 positively identified electrons were rejected. A total energy cut of 10(15) GeV for the 14(22) GeV run was applied to reject QED events escaping the above

cuts. Cosmics and 2γ events are very efficiently rejected by imposing a cut on the acoplanarity and acollinearity angles defined with $\mathbf{n}_1$ and $\mathbf{n}_2$ and the unit vectors of the incoming electron/positron directions $\mathbf{e}_1$ and $\mathbf{e}_2$:

$$\alpha_{\text{acoll}} = \cos^{-1}[-\mathbf{n}_1 \cdot \mathbf{n}_2]$$

$$\alpha_{\text{acop}} = \cos^{-1}\frac{(\mathbf{e}_1 \times \mathbf{n}_1)}{|\mathbf{e}_1 \times \mathbf{n}_1|} \cdot \frac{(\mathbf{e}_2 \times \mathbf{n}_2)}{|\mathbf{e}_2 \times \mathbf{n}_2|}.$$

The allowed range was $1.9° < \alpha_{\text{acoll}} < 60°$, $0.6° < \alpha_{\text{acop}} < 50°$. Background from low prong multihadronic events was removed by requiring the invariant mass m_i to be less than 2.1 GeV for each jet.

The angular acceptance for multiprong τ candidates was relaxed to the requirement that at least 2/3 of the charged particles in each hemisphere satisfy $|\cos\theta| < 0.85$. Each hemisphere was required to have an odd multiplicity with total charge balance. Acollinearity and acoplanarity cuts were imposed ($1° < \alpha_{\text{acoll}} < 50°$, $0.6° < \alpha_{\text{acop}} < 40°$) as well as a cut on the total energy ($0.6\,(1.)\,\text{GeV} < E_{\text{tot}} < 9.5\,(15)$ for 14(22) GeV, respectively). Furthermore an invariant mass cut of 2.1 GeV and a sphericity cut (0.14(0.1) for 14(22) GeV) were applied. Radiative QED events where the electron-positron pair from the γ conversion was not identified were rejected by requiring, for each jet, a minimal opening angle of 1.5° between the tracks in the plane containing the beam ($r\,z$ projection).

A total of 668 candidates were selected with the above criteria and subjected to visual scan. Residual multihadronic events and strongly showering QED events (both surviving the cuts due to incomplete reconstruction of mostly forward going tracks) were removed. At 14(22) GeV the number of $e^+e^- \to \tau^+\tau^-$ events retained was 178(182). Table 1 contains the number of $\tau^+\tau^-$ events, divided into the individual charged topologies. The over-all efficiency for the full solid angle is 37% for the $\tau^+\tau^-$ 2 prong and 49% for the $\tau^+\tau^-$ multiprong final states, as determined by a detailed Monte Carlo simulation of the reaction $e^+e^- \to \tau^+\tau^-$ in the CELLO detector (see below). Also given are the background events from multihadronic states for the respective topologies which could not be removed by the scan. All other backgrounds were found to be negligible. As a consistency check the topological branching ratios have been determined at both energies separately and compared to a previous measurement of the same experiment at higher energies [2]. The values found are given in Table 2 and are in excellent agreement with other experiments [3, 5]. For the branching ratio $\tau \to 5$ prongs + neutrals we obtain an upper limit of 0.9% by converting the one observed event into a 95% CL limit. This new value, although in agreement with other experiments, is in slight conflict with our earlier result [2].

Table 1. Observed charged topologies for $e^+e^- \to \tau^+\tau^-$. Also given is the background from multihadronic events (MUHA)

$\sqrt{s}$		Top.				
		1–1	1–3	3–3	1–5	
14 GeV	τ events	123	53	2	0	178
	MUHA	3.4	3.5	1.4	0.0	8.3
22 GeV	τ events	141	38	2	1	182
	MUHA	0.8	0.0	0.8	0.0	1.6
Total	τ events	264	91	4	1	360
	MUHA	4.2	3.5	2.2	0.0	9.9

Table 2. Topological branching ratios. Errors given are statistical (first) and systematic (second)

	$\sqrt{s} = 14$ [GeV]	$\sqrt{s} = 22$ [GeV]
$\tau \to 1$ prong + neutrals	$0.852 \pm 0.026 \pm 0.013$	$0.851 \pm 0.028 \pm 0.013$
$\tau \to 3$ prong + neutrals	$0.148 \pm 0.020 \pm 0.013$	$0.145 \pm 0.022 \pm 0.013$
$\tau \to 5$ prong + neutrals	< 0.01	< 0.01

Final State Analysis

Photon clean-up: For the further analysis of semihadronic decays of the τ we consider only decays with either a single charged prong acompanied by at least one neutral shower in the same hemisphere or 3 charged tracks (with or without additional neutrals). Due to the nature of hadronic showers from decay pions (and kaons) inside the liquid argon calorimeter not all neutral showers observed are genuine photons from a τ decay. Basically three sources exist for additional fake photons in the final state:

a) fluctuations of the hadronic shower initiated by charged decay hadrons which may result in 2 (or more) spatially separated showers inside the calorimeter,

b) charge exchange reactions creating π^0's inside the calorimeter leading to genuine electromagnetic showers,

c) bremsstrahlung of decay electrons in the beam pipe.

On the other hand genuine photons may be hidden by overlap with showers from charged particles or other photons. The observed neutral showers in a given hemisphere were thus submitted to a "clean up" procedure. In the following we describe only the most important cuts. Bremsstrahlung photons (in the one prong decay sample) were rejected by either

identifying the charged particle as an electron (see above) or by requiring an opening angle in the rz projection between the charged particle and the neutral shower of at least 1.5°. Neutral showers within a cone of 8° around a charged particle were counted as fake and thus removed if the fractional energy deposition in the last two lead layers ($>11\,X_0$) exceeded 50%. Earlier showers within the same cone were rejected if their energy did not exceed 60% of the charged particle's energy, assuming pion mass. Finally a minimum energy of 100 MeV and a minimal energy deposit of 70 MeV in the first 3 lead layers ($<11\,X_0$) was required for the photon candidates.

Table 3 shows the multiplicity distribution of the neutral showers before and after the photon clean-up, for 1 prong and 3 prong decays separately. One prong decays without neutral showers after the photon clean-up were not considered in the further analysis. The photon cuts described above were developed and monitored with data, using the decay $\tau \to \rho\nu$: candidates for this channel were selected from 1 prong decays with one or two additional photons in the same hemisphere. Due to the large momenta of the decay particles, the two photons from π^0 merge into one shower in about 45% of the ρ decays. Thus in addition to the 1 charged+2 photon final state also the 1 charged+1 photon topology was considered. The photon cuts were adjusted as to minimize the background in the invariant mass between the charged particle (assuming a pion) and the neutral shower(s), and to maximize the number of events in the ρ mass region. Figure 1a shows the invariant mass for the 1 charged+2 photon subsample with no analysis on the neutral showers and Fig. 1b the same distribution after the photon clean-up.

In order to determine the efficiencies with such detailed cuts on shower patterns we rely on Monte Carlo techniques giving special attention to simulate the processes under investigation as close as possible. In the Monte Carlo program we used a standard $\tau^+\tau^-$ generator [12] with initial state radiation. The produced τ's were allowed to decay according to the measured modes [3, 4]. Proper matrix elements were chosen for the leptonic decays ($\tau \to e\nu\nu$, $\mu\nu\nu$) and 2 body semihadronic decays ($\tau \to \pi\nu$, $\rho\nu$, $A_1\nu$). Multihadronic final states (4 and 5 pions) were modelled similar to the hadronic states from e^+e^- annihilation, as might be expected from CVC. All known resolutions and efficiencies for the individual detector components relevant to this analysis were incorporated. In particular, a realistic simulation of electromagnetic and hadronic showers in the liquid argon calorimeter was implemented using standard shower codes [13, 14]. The Monte Carlo events were subjected to the same reconstruction, selection and analysis procedures as the data, including visual scanning to evaluate systematic biases. The curves shown in the figures are results from our Monte Carlo simulation of the reaction (+backgrounds) under study.

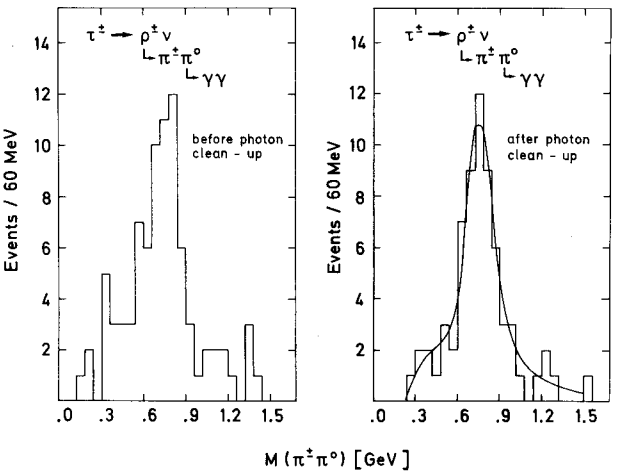

Fig. 1. Invariant mass of one charged pion+neutral showers. In a), neutral showers are not analysed for contributions of secondary hadronic interactions in the calorimeter, in b), the photon final state has been cleaned (see text). The Monte Carlo expectation is also drawn (curve)

Table 3. Neutral shower multiplicity distribution before (b) and after (a) the photon clean-up (see text)

Top.		$n(\gamma)$							
		0	1	2	3	4	5	6	7
1 prong	b	281	132	88	55	26	14	4	3
	a	308	122	91	52	15	12	0	0
3 prongs	b	23	38	11	9	4	1	0	0
	a	44	24	11	6	1	0	0	0

Branching ratios: It is evident from the previous discussion that a τ decaying into m charged pions, $2n$ photons (from $n\pi^0$'s)+ν will be found in various charged and neutral topologies: As far as the charged topology is concerned our algorithm for the identification of converted photons may fail to find the conversion pair due to measurement errors ($m+2$) or falsely identify a pion pair as an e^+e^- pair ($m-2$). Photons on the other hand may either escape detection because of overlap or limited acceptance, be rejected by the clean-up procedure, or be faked by a secondary interaction in the calorimeter and not be caught by the clean-up procedure. Thus in general one will have to solve a system of coupled

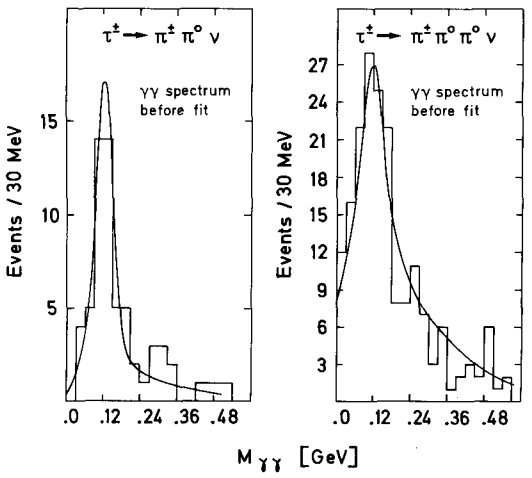

Fig. 2. $\gamma\gamma$ invariant mass distributions for the decays $\tau^{\pm} \to \pi^{\pm} \pi^0 \nu$ and $\tau^{\pm} \to \pi^{\pm} \pi^0 \pi^0 \nu$ (histograms). The Monte Carlo expectations are also drawn (curves)

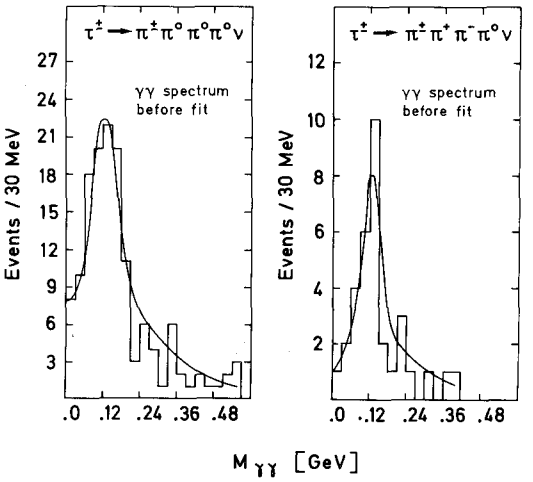

Fig. 3. $\gamma\gamma$ invariant mass distributions for the decays $\tau^{\pm} \to \pi^{\pm} \pi^0 \pi^0 \pi^0 \nu$ and $\tau^{\pm} \to \pi^{\pm} \pi^+ \pi^- \pi^0 \nu$ (histograms). The Monte Carlo expectations are also drawn (curves)

equations of the following form:

$$N_{ij} = \sum_{k,l} \varepsilon_{kl \to ij} N_{kl} \tag{7}$$

N_{ij} are the numbers of observed events (decays) with topology ij (ij could symbolize in an event, e.g., the charged multiplicity i in one jet and the charged multiplicity j of the other), N_{kl} is the number of events (decays) with topology kl, produced in 4π solid angle, and $\varepsilon_{kl \to ij}$ the probability to measure topology ij, when kl was produced in reality. The matrix elements $\varepsilon_{kl \to ij}$ have been calculated using Monte Carlo events. As an example we show in Table 4 the matrix elements used in calculating the topological branching ratios which are obtained by inversion of the matrix and are given in Table 2. The systematic errors are estimated by varying the cuts in the event- and topology-selection within reasonable limits and observing their effects on the branching ratios obtained.

Table 4. Efficiency Matrix $\varepsilon_{kl \to ij}$ for the determination of the correlated topological branching ratios at $\sqrt{s} = 14$ GeV (see text)

ij	kl			
	1−1	1−3	3−3	1−5
1−1	0.3584 ±0.0224	0.0157 ±0.0078	0.0024 ±0.0024	0
1−3	0.0056 ±0.0028	0.3804 ±0.0386	0.0816 ±0.0408	0.0168 ±0.0063
3−3	0	0	0.2653 ±0.0736	0.0024 ±0.0024
1−5	0	0	0	0.2518 ±0.0246

For the determination of the branching ratios with a given π^0 multiplicity we proceed in the following way: We neglect final states with more than 4 pions due to the small upper limit for its branching ratio measured in this experiment (the upper limit given in [5] is $<0.5\%$). For the final states with one charged particle we form three classes of decays, i.e. containing 1 or 2 photons (corresponding to $\pi\pi^0$), 3 or 4 ($\pi\pi^0\pi^0$), and more than 4 photons ($\pi\pi^0\pi^0\pi^0$). In order to minimize the expected feeddown from higher π^0 multiplicities we require for final states with 2 and 3 photons one successful fit to the π^0 mass (in the case of 3 photons we ask in addition for a minimal opening angle of 10^0 between the charged particle and the lone photon). For 4 photon final states we require a successful fit to $2\pi^0$'s. A probability cut of $>1\%$ was imposed for the fit. Final states with 3 charged particles are divided into 2 classes: events with no additional photons ($\pi\pi\pi$) and those with photons ($\pi\pi\pi\pi^0$). The $\gamma\gamma$ mass distributions for the various photon multiplicities are shown in Figs. 2 and 3. Clear π^0 signals with the expected widths are observed. We then calculate the probabilities $\varepsilon_{kl \to ij}$ for each of the 5 decay channels to end up in one of the observed classes. This matrix is given in Table 5. As can be seen from the table the off-diagonal elements for some channels are substantial. However, due to the more stringent cuts applied to the events for the determination of branching ratios, the matrix elements relating 1 and 3 prongs are very small ($|\varepsilon| < 0.001$) and therefore neglected. Inversion of this matrix, multiplied by the vector of observed decay

Table 5. Efficiency Matrix $\varepsilon_{kl\to ij}$ for the determination of the semihadronic branching ratios (see text)

ij	kl				
	$\pi\pi^0$	$\pi\pi^0\pi^0$	$\pi\pi^0\pi^0\pi^0$	$\pi\pi\pi$	$\pi\pi\pi\pi^0$
$1/1,2\gamma$	0.2583 $\pm$0.0114	0.1061 $\pm$0.0172	0.0296 $\pm$0.0063	0	0
$1/3,4\gamma$	0.0211 $\pm$0.0033	0.1397 $\pm$0.0198	0.0874 $\pm$0.0108	0	0
$1/>4\gamma$	0.0010 $\pm$0.0007	0.0140 $\pm$0.0062	0.1142 $\pm$0.0124	0	0
$3/0\gamma$	0	0	0	0.1724 $\pm$0.0214	0.0300 $\pm$0.0058
$3/>1\gamma$	0	0	0	0.0796 $\pm$0.0145	0.1654 $\pm$0.0135

classes yields the desired branching ratios. Systematic errors have again been estimated by varying all cuts involved in a systematic way and observing their influence on the branching ratios.

Results and Discussion

The branching ratios for reactions (1) to (5) are calculated using the matrix method as described in the previous chapter. It should be stressed that the branching ratios have been obtained independently of any assumptions on the total cross section for $e^+e^-\to\tau^+\tau^-$. Since charged hadrons are not identified in this experiment contributions from $\tau\to K^*\nu$ have to be substracted from the various topologies. The decay of $K^{*-}\to K^-\pi^0$ contaminates the channels (1) and (2), and $K^{*-}\to K^0\pi^-$ the channels (4) and (5) since no mass cut on the $\pi^+\pi^-$ system has been performed. Other contaminations from strange decay particles such as $\tau\to K\bar{K}\pi\nu$ are estimated to be very small [9] and have been neglected. The K^* contribution is substracted from the respective channels using the measured branching ratio [15].

The decay channel (1) is dominated by $\tau\to\rho\nu$ and we have tried to isolate the resonant and non-resonant contributions by introducting a mass cut at 1.3 GeV. We observe 5 events above that mass. After subtraction of the background (feed-down from higher π^0 multiplicities) we assume the same mass density from 1.3 GeV down to the ρ mass. The number of events thus estimated is then translated into the non-resonant contribution to the $\pi\pi^0$ decay channel.

The corrected branching ratios for all channels measured in this experiment are given in Table 6 together with those for $\tau\to e\nu\nu$, $\mu\nu\nu$, $\pi\nu$ as measured previously [4]. Since we redetermined $\tau\to\rho\nu$ in this experiment we are in a position to calculate a weighted average using our previous value [4]. This average is also given in the table. For completeness we added the measured branching ratios of the strange particle decay channels from another experiment [15] together with the particle data book values [16]. It should be stressed that the sum of the measured branching ratios now saturates the full width of the τ well within the experimental errors.

We have compared our results with predictions based on a standard coupling of the τ to the weak charged current [9, 10]. The predictions are usually given in terms of the partial widths into given channels. Apart from the decays $\tau\to e\nu\nu$, $\mu\nu\nu$, $\pi\nu$, $K\nu$ which can be calculated from first principles (knowing the pion decay constant and the Cabibbo angle) the decays into $2n$ pions are related to $e^+e^-\to 2n$

Table 6. Measured τ branching ratios and predictions

Decay channel	Experiment	Br (meas.) [%]	Pred. [%]	PDG [%]
$\tau\to e\nu\nu$	[4]	18.3 $\pm$2.4 $\pm$1.9	18.3	16.2 $\pm$1.0
$\tau\to\mu\nu\nu$	[4]	17.6 $\pm$2.6 $\pm$2.1	17.9	18.5 $\pm$1.2
$\tau\to\rho\nu$	[4]+this exp.	22.1 $\pm$1.9 $\pm$1.6	22.3	21.6 $\pm$3.6
$\tau\to\pi\pi^0\nu$ (non res.)	this exp.	0.3 $\pm$0.1 $\pm$0.3	very small	-
$\tau\to\pi\pi\pi\pi^0\nu$	this exp.	6.2 $\pm$2.3 $\pm$1.7	6.6	-
$\tau\to\pi\pi^0\pi^0\pi^0\nu$	this exp.	3.0 $\pm$2.2 $\pm$1.5	1.1	-
$\tau\to\pi\nu$	[4]	9.9 $\pm$1.7 $\pm$1.3	10.8	10.7 $\pm$1.6
$\tau\to\pi\pi\pi\nu$	this exp.	9.7 $\pm$2.0 $\pm$1.3	upper limit 18.7 ($15.4\,\pi\rho$)	7.0 $\pm$5.0 ($5.4\pm1.7, \pi^-\rho^0$)
$\tau\to\pi\pi^0\pi^0\nu$	this exp.	6.0 $\pm$3.0 $\pm$1.8		
$\tau\to\pi\pi\pi\pi\pi\nu$	this exp.	<0.9	0.9	-
	[5]	<0.5		
$\tau\to K\nu$	[15]	1.3 $\pm$0.5	0.5	-
$\tau\to K^*\nu$	[15]	1.7 $\pm$0.7	1.3	1.7 $\pm$0.7
$\tau\to K\pi\pi\nu$			1.5	-

pions using the CVC hypothesis [9]:

$$\Gamma(\tau \to \nu + 2n\pi) = \frac{G^2}{(2\pi)^2 (2M_\tau)^3} \frac{\cos^2 \theta_c}{4\pi^2 \alpha^2}$$
$$\cdot \int (M_\tau^2 - q^2)^2 (M_\tau^2 + 2q^2) q^2 \sigma(e^+ e^- \to 2n\pi) dq^2. \quad (8)$$

Here, G is the Fermi coupling constant, θ_c the Cabibbo angle and α the fine structure constant. The integral over the $e^+ e^-$ cross section is taken from the $2n$ pion threshold to the τ mass M_τ.

Using data from $e^+ e^-$ measurements the authors of [9] have derived the partial widths for $n = 1, 2$ (the data for $n = 3$ show an effective threshold at 2 GeV and thus do not contribute). $\tau \to K^* \nu$ is derived from $\rho \nu$ using Cabibbo suppression. Calculations of the axial current contribution (3 and 5 pions) have to rely on certain model assumptions like PCAC or current algebra to predict the "hard pion" final states such as $\tau \to 3\pi \nu$, or use soft pion theorems to arrive at $\tau \to 5\pi \nu$ [9, 10]. Since these predictions seem to be less certain compared to the vector part and also diverge in the literature we have chosen the alternative way to estimate the axial component by saturation: Summing up all "well-known" partial widths and normalizing the partial width for $\tau \to e \nu \nu$ to the branching ratio measured by CELLO [4] we predict an upper limit for Br $(\tau \to 3\pi \nu)$ which is given in Table 6. The result from a specific resonance model [9, 10] for Br $(\tau \to 3\pi \nu)$ is also shown.

We find good agreement between experiment and the predictions from the standard $V-A$ coupling of a heavy sequential lepton. For the first time, the decay $\tau \to 4\pi \nu$ in its 2 charge combinations has been measured, opening up a new test for CVC so far only possible with the decay $\tau \to \rho \nu$. Comparing to the predictions we find good agreement with CVC. Concerning the axial coupling, both the saturation assumption and specific models with resonance dominance agree with the measured overall branching ratio $\tau \to 3\pi \nu$. No more detailed theoretical predictions for the ratio Br $(\tau \to \pi\pi\pi\nu)$/Br$(\tau \to \pi\pi^0\pi^0\nu)$ are available. It should be noted, however, that a purely resonant channel such as $\tau \to A_1 \nu$ would yield a ratio of 1, not far from our measured value.

Acknowledgement. We are indebted to the PETRA machine group and the DESY computer center for their excellent support during the experiments. We acknowledge the invaluable effort of all engineers and technicians of the collaborating institutions in the construction and maintenance of the apparatus, in particular the operation of the magnet system by G. Mayaux and Dr. Horlitz and their groups. The visiting groups wish to thank the DESY directorate for the support and kind hospitality extended to them. This work was partly supported by the Bundesministerium für Forschung und Technologie.

References

1. S.L. Glashow: Nucl. Phys. **22**, 579 (1961); S. Weinberg: Phys. Rev. Lett. **19**, 1264 (1967); A. Salam: Proceedings of the 8th Nobel Symposium. Stockholm: Almqvist and Wiksell 1968
2. CELLO Collab., H.J. Behrend et al.: Phys. Lett. **114 B**, 282 (1982)
3. MARK J Collab., B. Adeva et al.: Phys. Rev. Lett. **48**, 1701 (1982); D.P. Barber et al.: Phys. Lett. **95 B**, 149 (1980); JADE Collab., W. Bartel et al.: Phys. Lett. **108 B**, 140 (1982); Phys. Lett. **99 B**, 281 (1981); CELLO Collab., H.J. Behrend et al.: Z. Phys. C - Particles and Fields **16**, 301 (1983); PLUTO Collab., Ch. Berger et al.: Z. Phys. C - Particles and Fields **7**, 289 (1981); TASSO Collab., R. Brandelik et al.: Phys. Lett. **117 B**, 365 (1982); Phys. Lett. **110 B**, 173 (1980); MAC Collab., E. Fernandez et al.: Phys. Rev. Lett. **50**, 1238 (1983). For a review see e.g. M. Davier, Proceedings of the 21st International Conference on High Energy Physics, p. c3-471 (1982) Paris
4. CELLO Collab., H.J. Behrend et al.: Phys. Lett. **127 B**, 270 (1983)
5. MARK II Collab., C.A. Blocker et al.: Phys. Rev. Lett. **49**, 1369 (1982); Phys. Rev. Lett. **109 B**, 119 (1982)
6. DELCO Collab., W. Bacino et al.: Phys. Rev. Lett. **42**, 6 (1979)
7. MARK II Collab., G.J. Feldman et al.: Phys. Rev. Lett. **48**, 66 (1982); MAC Collab., W.T. Ford et al.: Phys. Rev. Lett. **49**, 106 (1982); CELLO Collab., H.J. Behrend et al.: Nucl. Phys. **B 211**, 369 (1983)
8. PLUTO Collab., G. Alexander et al.: Phys. Lett. **78 B**, 162 (1978)
9. H.B. Thacker, J.J. Sakurai: Phys. Lett. **36 B**, 103 (1971); Y.S. Tsai: Phys. Rev. **D 4**, 2821 (1971); F.J. Gilman, D.H. Miller: Phys. Rev. **D 17**, 1846 (1978); N. Kawamoto, A.I. Sanda: Phys. Lett. **76 B**, 446 (1978)
10. T.N. Pham, C. Roiesnel, T.N. Truong: Phys. Lett. **78 B**, 623 (1978)
11. CELLO Collab., H.J. Behrend et al.: Phys. Scr. **23**, 610 (1981); H.J. Behrend: Comp. Phys. Commun. **22**, 365 (1981)
12. F.A. Berends, R. Kleiss: Nucl. Phys. **B 186**, 22 (1981)
13. R.L. Ford, W.R. Nelson: EGS code, SLAC Report 210 (1978)
14. RSIC Comp. Code. Collab., HETC code, Oak Ridge National Laboratory, CCC 178
15. MARK II Collab., J.M. Dorfan et al.: Phys. Rev. Lett. **46**, 215 (1981); G.S. Abrams et al.: Phys. Rev. Lett. **48**, 1586 (1982)
16. Review of Particle Properties: Phys. Lett. **111 B**, 1 (1982)